Project 2

Active Automotive Suspension Design

A Report Submitted in Partial Fulfillment of the Requirements for SYDE 352.

Group Number 6 (Wednesday)

Yazan Obeidi

Faculty of Engineering
Department of Systems Design Engineering

April 3 2017
Professor: Nasser Lashgarian Azad

Table of Contents

Abstract....2
1 Systems Model....3
2 Physical Equations....3
3 Open Loop Response....5
    3.1 Level Step Disturbance....6
    3.2 Pothole Disturbance....7
    3.3 Sinusoidal Bumpy Disturbance....8
    3.4 Random Disturbance....10
4 Controller Design....11
    4.1 Desired Performance Characteristics....11
        4.1.1 Desired Performance Specifications....12
        4.1.1 Desired Closed Loop Poles....13
    4.2 PID Controller Design....13
        4.2.1 Root Contour Method....13
5 Results and Comparisons....14
    3.1 Level Step Disturbance....14
    3.2 Pothole Disturbance....14
    3.3 Sinusoidal Bumpy....15
        3.2.1 Varying Amplitude....15
        3.2.2 Varying Frequency....15
    3.4 Random Disturbance....16
6 Conclusions and Recommendations....16
References....18
Appendix A....19
Appendix B....20

Abstract

Active vehicular suspension systems are used enhance the performance of passive suspension systems by providing a dynamic response to road disturbance in both performance and comfort. In this report a passive quarter-car active suspension system is modeled and simulated in Simulink against several types of road profiles: level-step, pothole, sinusoidal bumpy, and random. Next, desired performance specifications are defined and an appropriate PID controller for a hydraulic actuator is developed using Root Contour method. Three design iterations are performed and the resulting active suspension system is evaluated and compared against the performance of the passive case. Reduced overshoot and settling time are observed that fall within desired performance specifications indicating success in the PID controller and the root locus iterations. However upon considering sprung mass dynamics in greater detail, evidence suggests that improved suspension travel is a trade off with increased sprung mass dynamics for the given system parameters. It is recommended that the unsprung spring stiffness is increased, or the sprung mass to unsprung mass ratio is increased such that the actuator has a greater response on the unsprung mass. It is also recommended that the maximum actuator force allowance be increased as saturation in the actuator response is visible in a majority of cases.

1 Systems Model

Shown below is a quarter-car model of a passenger sedan outfitted with an active suspension system.

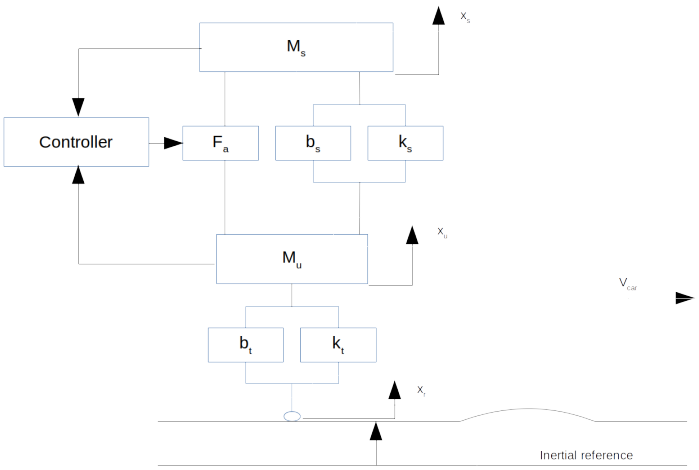

Figure 1: Quarter Car with Active Suspension Systems Model

Params.	Unit	Value
M_s	kg	350
M_u	kg	60
k_s	$\frac{N}{m}$	17500
k_t	$\frac{N}{m}$	175000
b_s	$\frac{Ns}{m}$	1300
b_t	$\frac{Ns}{m}$	0
F_a max	N	3500

Table 1: System Parameters

The first step in developing a controller for the actuator to enhance the passive suspension components includes taking a free body diagram to develop physical equations:

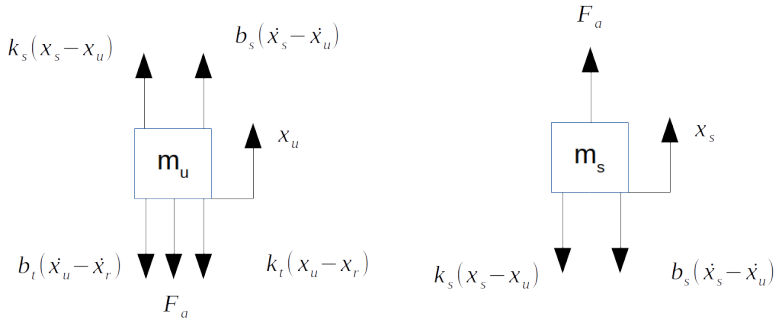

Figure 2: Free Body Diagram

2 Physical Equations

The two masses in Figure 2 may be described by the following differential equations by Newton's second law:

$$F_a - b_s(\dot{x}_s - \dot{x}_u) - k_s(x_s - x_u) = m_s\ddot{x}_s \quad (1)$$

$$b_s(\dot{x}_s - \dot{x}_u) + k_s(x_s - x_u) - b_t(\dot{x}_u - \dot{x}_r) - k_t(x_u - x_r) - F_a = m_u\ddot{x}_u \quad (2)$$

Take the Laplace transform of Eq. 1 and 2 and re-arrange to develop transfer functions relating $X_s(s)-X_u(s)$ with each of $F_a(s)$ and $X_r(s)$:

$$(m_s s^2+b_s s+k_s)X_s(s)-(b_s s+k_s)X_u(s)=F_a(s) \quad (3)$$

$$-(b_s s+k_s)X_s(s)+(m_u s^2+(b_s+b_t)s+(k_s+k_t))X_u(s)=(b_t s+k_t)X_r(s)-F_a(s) \quad (4)$$

The system of equations may be expressed in matrix form:

$$\begin{bmatrix}(m_s s^2+b_s s+k_s) & -(b_s s+k_s)\\ -(b_s s+k_s) & (m_u s^2+(b_s+b_t)s+(k_s+k_t))\end{bmatrix}\begin{bmatrix}X_s(s)\\ X_u(s)\end{bmatrix}=\begin{bmatrix}F_a(s)\\ (b_t s+k_t)X_r(s)-F_a(s)\end{bmatrix} \quad (5)$$

Note that Eq. 5 is in the form $A\vec{x}=\vec{b}$, where

$$A=\begin{bmatrix}(m_s s^2+b_s s+k_s) & -(b_s s+k_s)\\ -(b_s s+k_s) & (m_u s^2+(b_s+b_t)s+(k_s+k_t))\end{bmatrix} \quad (6)$$

So that if A is non-singular,

$$\vec{x}=A^{-1}\vec{b} \quad (7)$$

Applying Eq. 7:

$$det(A)=(m_u s^2+(b_s+b_t)s+(k_s+k_t))(m_s s^2+b_s s+k_s)-(b_s s+k_s)(b_s s+k_s) \quad (8)$$

$$\begin{bmatrix}X_s(s)\\ X_u(s)\end{bmatrix}=\frac{1}{det(A)}\begin{bmatrix}(m_u s^2+(b_s+b_t)s+(k_s+k_t)) & (b_s s+k_s)\\ (b_s s+k_s) & (m_s s^2+b_s s+k_s)\end{bmatrix}\begin{bmatrix}F_a(s)\\ (b_t s+k_t)X_r(s)-F_a(s)\end{bmatrix} \quad (9)$$

Finally, Eq. 9 can be further simplified to:

$$\begin{bmatrix}X_s(s)\\ X_u(s)\end{bmatrix}=\frac{1}{det(A)}\begin{bmatrix}(m_u s^2+b_t s+k_t) & (b_s b_t s^2+(b_s k_t+b_t k_s)s+k_s k_t)\\ -m_s s^2 & (m_s b_t s^3+(m_s k_t+b_s b_t)s^2+(b_s k_t+b_t k_s)s+k_s k_t)\end{bmatrix}\begin{bmatrix}F_a(s)\\ X_r(s)\end{bmatrix} \quad (10)$$

From Eq. 10, two transfer functions $P(s)$, which relates suspension travel to actuator force, and $Q(s)$, which relates suspension travel to the road profile, can be formulated by taking $X_r(s)=0$ and $F_a(s)=0$ respectively, resulting in:

$$P(s)=\frac{X_s(s)-X_u(s)}{F_a(s)}=\frac{(m_s+m_u)s^2+b_t s+k_t}{det(A)} \quad (11)$$

$$Q(s)=\frac{X_s(s)-X_u(s)}{X_r(s)}=\frac{-m_s b_t s^3-m_s k_t s^2}{det(A)} \quad (12)$$

An additional transfer function $G_s(s)$ may be developed for the sprung mass displacement X_s and another $G_t(s)$ for the tire deflection X_u for when $F_a(s)=0$:

$$G_s(s)=\frac{X_s(s)}{X_r(s)}=\frac{(b_s b_t s^2+(b_s k_t+b_t k_s)s+k_s k_t)}{det(A)} \quad (13)$$

$$G_t(s)=\frac{X_u(s)}{X_r(s)}=\frac{(m_s b_t s^3+(m_s k_t+b_s b_t)s^2+(b_s k_t+b_t k_s)s+k_s k_t)}{det(A)} \quad (14)$$

Similarly for when $X_r(s)=0$:

$$G_s'(s)=\frac{X_s(s)}{F_a(s)}=\frac{m_u s^2+b_t s+k_t}{det(A)} \quad (15)$$

$$G_t'(s)=\frac{X_u(s)}{F_a(s)}=\frac{-m_s s^2}{det(A)} \quad (16)$$

Eq. 8 and 11-16 with substituted numerical values can be found in Appendix A.

Note the zeros of $det(A)$ are all in the left-hand plane (LHP) indicating naturally stable systems for all derived transfer functions above. Also note that Eq. 11 and 12 can be described by Eq. 13-16:

$$P(s)=G_s(s)-G_t(s) \quad (17)$$

$$Q(s)=G_s'(s)-G_t'(s) \quad (18)$$

Eq. 17 and 18 will be useful when simulating the entire closed-loop system in section 4.0. These additional relationships will enable evaluation of tire deflection and sprung mass dynamics in addition to suspension travel allowing for richer comparisons to be made between the active and passive cases.

3 Open Loop Response

The open-loop response of the system is the output of $Q(s)$ subjected to perturbations from changes in the road profile, $X_r(s)$. In the open loop case, $F_a(s)=0$, meaning the passive suspension model is as follows:

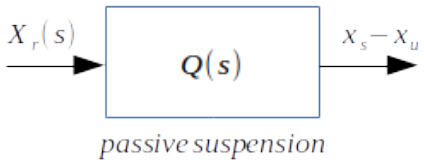

Figure 3: Open loop suspention model, $F_a=0$

As noted above, the poles of $Q(s)$ are all in the LHP indicating open-loop stability. To test this hypothesis and to explore the dynamics of the passive system, various road profiles are subjected to a computational simulation created in Simulink and the resulting effects on the suspension travel, sprung mass displacement and acceleration, and tire deflection are observed. To observe the latter two phenomenon, Eq. 13 and 14 are employed.

3.1 Level Step Disturbance

A common road disturbance can be a level step in the road, where the profile shifts from one constant to another, i.e. a step input disturbance. On a typical road these imperfections rarely exceed values greater than one or two decimeters, certainly not greater than half a metre or a metre or the road would close for maintenance. Applying a 10cm, 15cm and 20cm step disturbance input at 1 second produces the responses shown in Figure 4, with the input shown in the bottom scope:

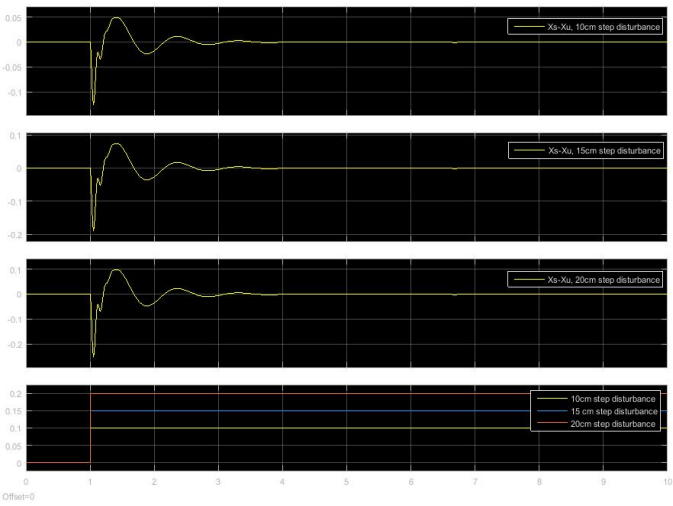

Figure 4: Open loop suspension travel for 10cm, 15cm and 20cm step disturbances

Fortunately the output responses shown above matches intuition. The response is stable and sinusoidal by nature, shown by the decaying oscillations between 2-4 seconds. The suspension travel, for each positive step disturbance case, is shown to rapidly compress and then expand with about a 12% overshoot compared to the input disturbance, with compression magnitudes that slightly exceed the magnitude of the step disturbance. The under-damped system has a quick rise time of approximately 0.05 seconds and settles back to the equilibrium of within 3 seconds after perturbation. In general the suspension system did not successfully absorb the initial perturbation, as in general the first overshoot exceeds the magnitude of the input, and the second overshoot is about half the magnitude of the initial input. Yet the passive system certainly did dissipate the initial displacement reasonably quickly in the

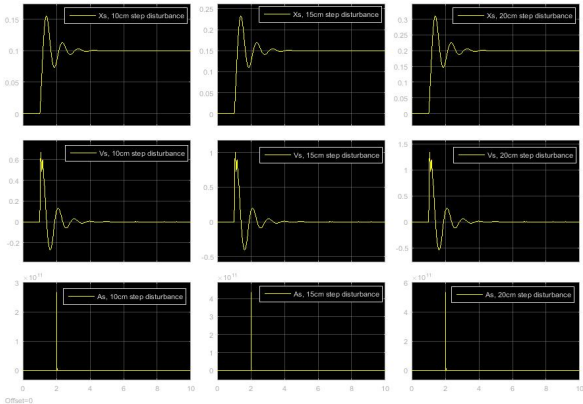

Figure 5: Open loop sprung mass dynamics for 10cm, 15cm and 20cm disturbances

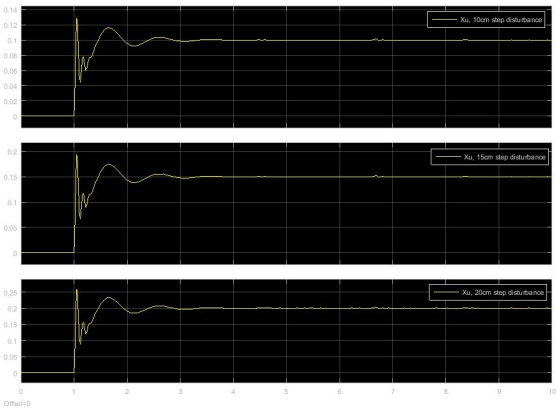

Figure 6: Open loop tire deflection for 10cm, 15cm and 20cm disturbances

order of a few seconds. An interesting feature is the small oscillation between the global minimum and maximum of the response. This is likely a feature resulting from the coupled interaction between the two masses.

Plotting the sprung mass displacement, velocity, and acceleration for the same step input disturbances results in the plots above.

In Figure 5, similarly as before an identical but scaled response is observable between the outputs of the different amplitude step disturbances. About a 50% overshoot is visible in all displacement signals. Compared to the suspension travel which naturally settled back to its original equilibrium, the sprung mass displacement, as well as the tire deflection in Figure 6, maintains its deformation as long as the disturbance signal exists. Notably is the acceleration of the sprung mass displacement which has an very large near-instantaneous peak at the time of perturbation. It is likely that the riders on board the vehicle will notice the jerk due to the rapid rate of change of acceleration, and combined with the large magnitude of acceleration will feel increasingly uncomfortable as the step size in the road increases.

3.2 Pothole Disturbance

A second common road imperfection are pothole type disturbances. These imperfections are similar to step imperfections but return back to equilibrium fairly rapidly; a pothole can be considered as two step inputs, one after the other. Simulation of the passive suspension system with this type of road profile is shown in Figure 7. Looking at the falling edge of the pothole signal, the negative step disturbance produces an identical behaviour as the step disturbance but reflected about the x-axis, which is expected. At the rising edge of the pothole similar response as the step disturbance is also noted. Considering that the system is linear time-invariant (LTI) it makes sense that the pothole, which is simply two consecutive step disturbances, produces behaviour that corresponds with two consecutive step disturbances. It follows that similar dynamics are observed: the system has a rapid rise time of about 0.05 seconds, settles in under 3 seconds after the final change in road profile, has peak overshoots with magnitudes greater than the change in road profile, and returns back to the initial equilibrium.

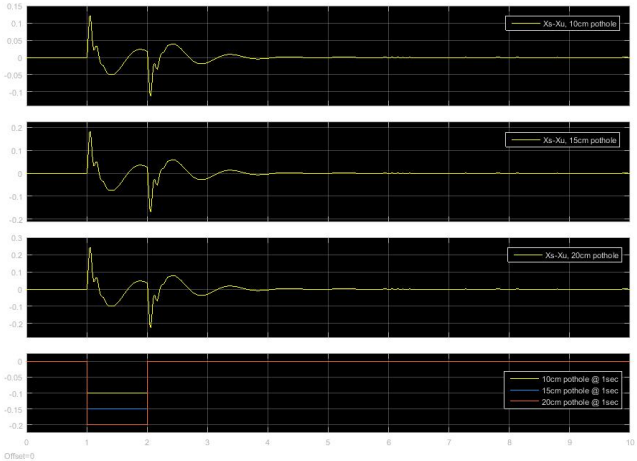

Figure 7 : Open loop suspension travel for 10cm, 15cm and 20cm deep pothole @ 1sec

Similarly with the sprung mass dynamics and tire deflection the pothole response is simply the sum of two consecutive step input responses obtained in section 3.1:

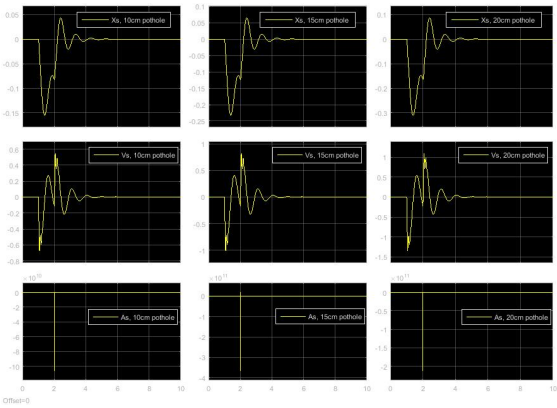

Figure 8:Open loop sprung mass dynamics , 10cm, 15cm and 20cm deep pothole @ 1s

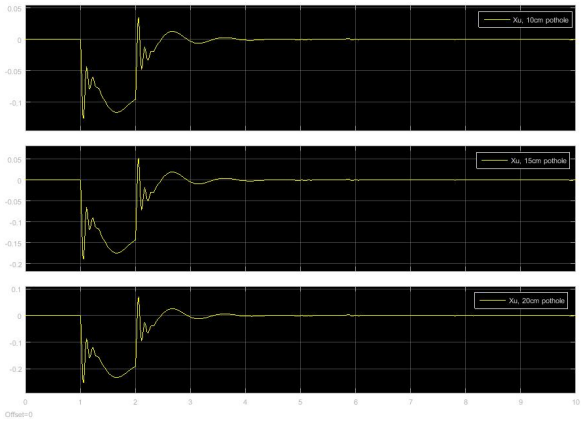

Figure 9: Open loop tire deflection for 10cm, 15cm and 20cm deep pothole @ 1sec

In this case, the suspension travel in addition to the sprung mass displacement and tire deflection return to their initial equillibrium positions as the road profile returns to zero. In total the system undergoes transient behaviour for about 3 seconds after the start of the pothole disturbance with a 15% maximum overshoot. Again it is clear that the pothole result is the superposition of both rising edge and falling edge cases of the previous level step disturbance. In general the passive system has satisfactory performance in the pothole case due to the high overshoot, somewhat long settling time and no steady-state error.

3.3 Sinusoidal Bumpy Disturbance

A third common road disturbance is when the form takes a sinusoidal bumpy shape, such as an eroded road, a set of speed bumps, rumble strips on the side of highways, or deposits of mud or snow taking on a shape that fluctuates in height along the path of the vehicle. A sinusoidal type disturbance can be the result of several constituent perturbations of varying amplitude and frequency. Exploring the effects of changing the amplitude of a 14 rad/s sinusoidal disturbance from 0-2 seconds:

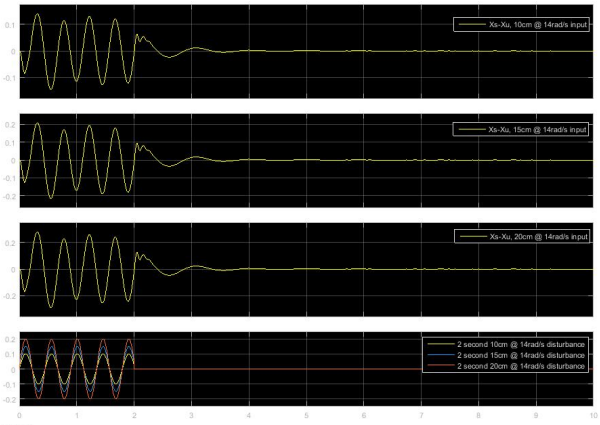

Figure 10: Open loop suspension travel for 10cm, 15cm and 20cm amplitude disturbances at 14rad/s for 2 sec

In the above response for the 10cm amplitude perturbation, the first five overshoot values have amplitudes of the following magnitude: 0.9, 0.12. 0.13, 0.11, 0.11. It is clear that the overshoot increases and decreases in value suggesting resonant effects between the driving input and the system.

This is the same phenomenon observed in the previous disturbance cases when the response signal magnitude exceeds that of the input signal magnitude.

Looking at also the open loop sprung mass dynamics and tire deflection, the same conclusions as before can be made: the results are simply scaled correspondingly as the input magnitudes are

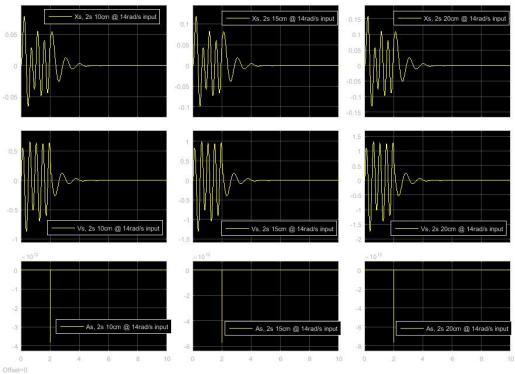

Figure 11: Open loop sprung mass dynamics for 10cm, 15cm and 20cm step disturbances

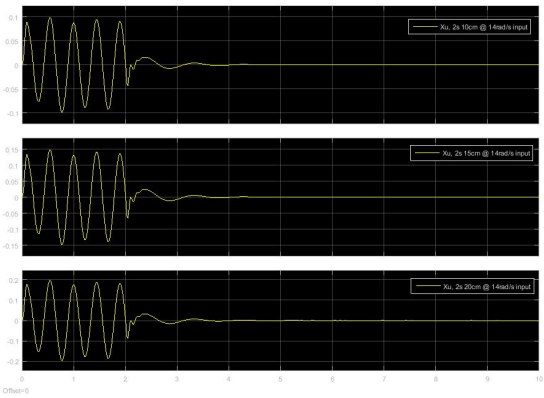

Figure 12: Open loop tire deflection for 10cm, 15cm and 20cm step disturbances

increased. Clearly during the transient portion of the response when the system is undergoing changes from the road profile there is essentially no damping, in fact there is some small amount of constructive interference. When the input signal is stopped, the system however returns to equilibrium within about 2 seconds. What this means to the passengers on board the vehicle is that they will feel the full magnitude of the oscillations but relatively soon afterwards they will be settled back at equilibrium. All oscillations are damped within about 2 seconds and maintain no steady-state error.

Varying frequency, on the other hand, produces some more interesting results. At 20rad/s and 14 rad/s, a 10cm amplitude wave produces a noticeable consistent constructive interference. However at 7 rad/s the constructive interference builds up over the four seconds of driving time to exceed over twice the input magnitude. Clearly the system resonant frequency is around 7 rad/s. Similarly as before all oscillations are damped within about 2 seconds.

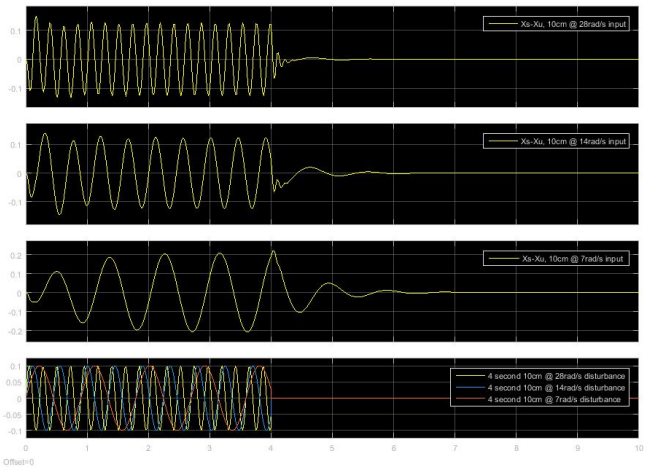

Figure 13: Open loop suspension travel for 10cm amplitude disturbances at 28, 14 and 7rad/s for 4 sec

Looking at the sprung mass displacement, there is a clear positive correlation in magnitude as the input frequency is decreased. At 28 rad/s other than the initial overshoot there are around 2cm displacements. At 14 rad/s the displacements are about 6cm. However at 7 rad/s the displacements are nearly 20 cm. Tire deflection on the other hand is the complete opposite – at 7 rad/s there is substantial damping, whereas at 28 rad/s it looks essentially undamped. This suggests that 7 rad/s is near the resonant frequency for only the sprung mass portion and not the tire.

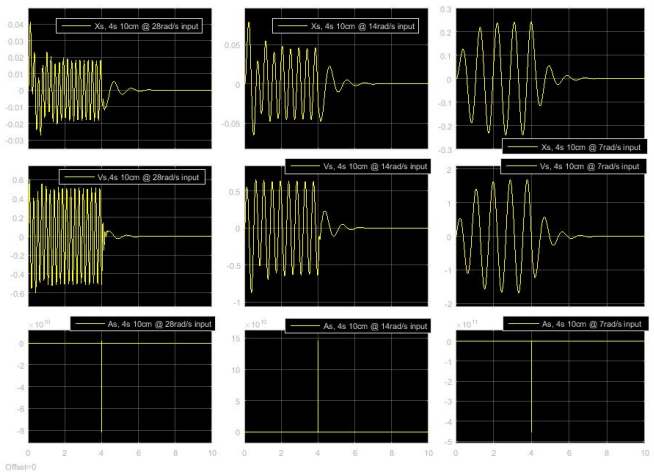

Figure 15: Open loop sprung mass displacement for 10cm amplitude disturbances at 28, 14 and 7rad/s for 4 sec

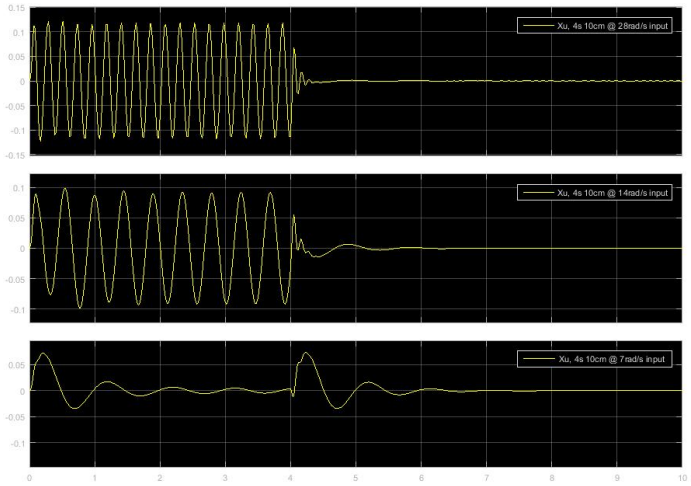

Figure 14: Open loop tire deflection for 10cm amplitude disturbances at 28, 14 and 7rad/s for 4 sec

3.4 Random Disturbance

Finally, the last class of likely road disturbances are random disturbances. These can be due to numerous factors such as waste on the road, for example tree leaves and branches, tire pieces, or plastic bottles, imperfections in road construction, or road material, for example when driving on a gravel road. Below is the response of the passive suspension system when subjected random inputs of increasing magnitude. Similarly as with all other disturbances since the system is LTI, a scaled input produces the identical scaled output. The system is naturally damped within about 2 seconds.

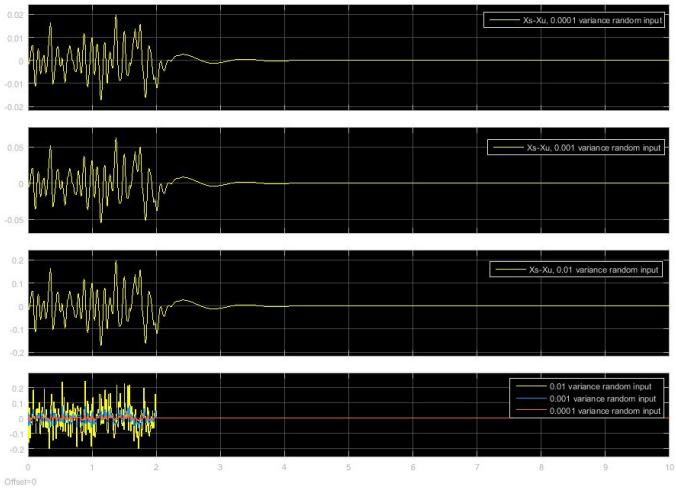

Figure 16: Open loop suspension travel for 0.0001, 0.001, 0.01 variance random input for 2 sec

For the sake of brevity, the sprung mass dynamics and tire deflection plots are omitted for the random disturbance signal, however the tire deflection response takes nearly the same form as the suspension travel and the sprung mass dynamics follow the same trend as all other disturbances: a large instantaneous acceleration and an displacement magnitude that corresponds with disturbance size.

4 Controller Design

The system of interest is comprised of two LTI components: the active suspension component driven by the actuator, and the passive suspension component due to perturbations from the road profile, defined as $P(s)$ and $Q(s)$ respectively. By the principle of superposition, they may be combined into a single model representative of the complete quarter car active suspension system:

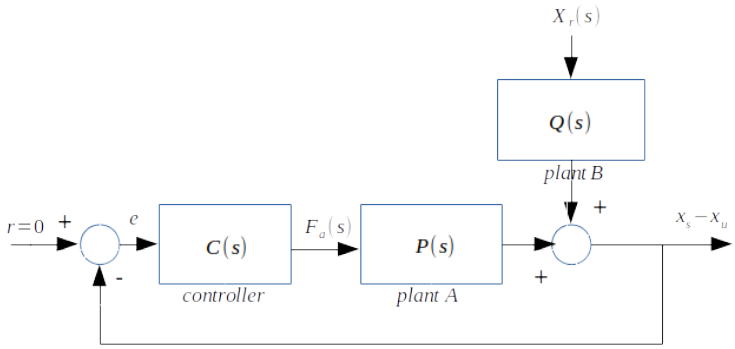

Figure 17: Closed Loop System Block Diagram

The block diagram above can be described by the following closed loop transfer function for when there is no external disturbance:

$$T_{cl} = \frac{C(s)P(s)}{1 + C(s)P(s)} \quad (19)$$

And for a Proportional Integral Derivative (PID) controller,

$$C(s) = \frac{k_p s + k_d s^2 + k_i}{s} \quad (20)$$

Note: to be able to observe the direct effects on the suspension travel $X_s(s) - X_u(s)$ in addition to the sprung mass displacement $X_s(s)$ and tire deflection $X_u(s)$ individually, Eq. 24 and 25 are used in the Simulink model instead of Eq. 11 and 12. Ultimately this does not affect the results but allows for greater insight into system dynamics as a comparison of sprung mass dynamics and tire behaviour can be made in addition to suspension dynamics, when comparing the active case against the passive case.

4.1 Desired Performance Characteristics

A good active suspension system minimizes the effects of disturbances while still providing satisfactory handling and maneuverability, and thus, safety [1, 2].

Considering the results of the open-loop passive system, several opportunities for improvement are evident. Reducing the overshoot of the suspension travel, sprung mass and tire deflection would increase passenger comfort [1]. Reducing the large peak acceleration of the sprung mass would also

increase ride comfort [3]. Both of these cases correspond to the damping of the system: increased damping would reduce the maximum overshoots and the sprung pass acceleration. Too much, however and the system will transfer much of the road disturbance increasing rider discomfort; too little and the stability of the vehicle, particularly while turning at higher speeds, is compromised [4]. As the suspension travel is simply the difference between the tire displacement and sprung mass displacement, minimizing their overshoots would result in a smaller suspension travel. In the simulated open-loop cases about a 50% maximum overshoot for the sprung mass and 20% maximum overshoot for the tire deflection was found.

Observing the responses in the open-loop cases it also is possible to see that the passive system consistently produces a settling time of about 3 seconds for all input disturbances. A decreased settling time would reduce the interval of passenger discomfort increasing ride quality.

Figure 18: Solution Regions for overshoot and settling time specifications

Steady-state error is not visible on any of the passive suspension system responses in the previous section therefore no steady-state error specification is defined for the active controller. Therefore the characteristics described result in a solution region that is the combination of s-planes in Figure 18.

4.1.1 Desired Performance Specifications

Specific values for maximum overshoot and settling time depend on the vehicle and its passive suspension system, the expected road profile, and the purpose of the vehicle. For example a sports car would likely have a stiffer suspension system than a family sedan, as a primary objective would be speed instead of comfort. Therefore for the purposes of formulating a PID controller, assume that the purpose of this system is a family sedan where comfort, and therefore low acceleration in the sprung mass as well as relatively low suspension travel is desired.

As current state-of-the-art research suggests possible reductions of more than half of overshoot for similar quarter-car models [1, 2, 4], try settling the desired maximum overshoot to about 1/3 of what it currently is, or 15%.

For settling time which is generally observed as 3 seconds for the passive case, aim for a similar reduction to about 1.25 seconds for 1% settling time.

1. Maximum overshoot of 15% given a unit step impulse
2. 1% settling time of 1.25 seconds given a unit step impulse.

4.1.1 Desired Closed Loop Poles

The desired closed loop poles for a second order closed loop transfer function take the following form [5]:

$$s_{d1,2} = -\sigma \pm j\,\omega_d \quad (21)$$

Where

$$\sigma = \zeta\,\omega_n \quad \text{and} \quad \omega_d = \omega_n\sqrt{(1-\zeta^2)} \quad (23, 24)$$

Therefore

$$s_{d1,2} = -\zeta\,\omega_n \pm j\,\omega_n\sqrt{(1-\zeta^2)} \quad (25)$$

A second order approximation of the desired closed loop poles will be used despite that the characteristic equations of all transfer functions is to the 4th degree. This simplification will result in an easier target for root locus iteration, and will still ultimately produce a viable controller.

Using Figure 3-24 in Feedback Control of Dynamic Systems [5] it is found that for a 15% or less maximum overshoot specification, $\xi = 0.5$.

Using 2nd Order System Transient Response equations for a step input as an approximation [5]:

$$t_s = \frac{4.6}{\sigma} \rightarrow \sigma = \frac{4.6}{1.25} = 3.68 \quad (26)$$

Combining the values for both specifications the desired closed loop poles are obtained:

$$s_{d1,2} = -3.68 \pm 6.374\,j \quad (27)$$

4.2 PID Controller Design

Combine Eq. 11, 19 and 20 to obtain the closed loop transfer function for suspension travel:

$$T_{cl} = \frac{C(s)P(s)}{1+C(s)P(s)} = \frac{(k_p s + k_d s^2 + k_i)[(m_s+m_u)s^2 + b_t s + k_t]}{s\,det(A) + (k_p s + k_d s^2 + k_i)[(m_s+m_u)s^2 + b_t s + k_t]} \quad (28)$$

Simplifying the denominator of T_{cl} produces the resulting characteristic equation (Eq 29):

$$m_u m_s s^5 + (k_d(m_s+m_u) + m_u b_s + b_s b_t)s^4 + (m_u k_s + b_s b_t + (k_s+k_t)m_s + k_p(m_s+m_u) + k_d b_t)s^3 + (2k_s b_t + b_t k_p + k_d k_t + k_i(m_s+m_u))s^2 + (k_t k_p + b_t k_i + k_t k_s)s + k_t k_i = 0$$

4.2.1 Root Contour Method

Root contour method is used to systematically determine PID values that results in an active suspension system that fits within the desired performance criteria. Two root contour iterations are shown in Appendix B, however a total of three iterations where performed to develop an appropriate PID controller as follows:

$$C(s) = \frac{3575\,s^2 + 22230\,s + 47330}{s}$$

5 Results and Comparisons

3.1 Level Step Disturbance

The level-step disturbance is not shown as the pothole disturbance is the superposition of two level-step disturbances as shown in Section 2.

3.2 Pothole Disturbance

In Figure 19 the suspension travel is shown for the closed loop active suspension response to various sized potholes. There is an improvement in peak overshoots, about 1% for both of the rising and falling edge of the pothole, particularly for the $10\,cm$ case where the amplitude of the response is within $\pm 10\,cm$, whereas in the open loop case the suspension travel was about 12cm. In addition, an improvement in settling time is observed; the suspension travel returns back to equilibrium in about 1.5 seconds which meets the settling time desired performance specification. Actuator force for the 10cm pothole is shown in Figure 19; the actuator reaches saturation twice, at the peaks of the road profile.

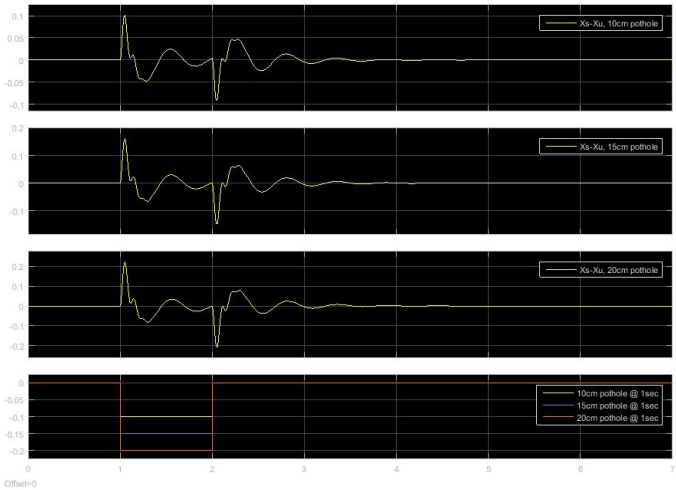

Figure 19: Closed loop suspension travel for 10, 15, 20cm deep pothole

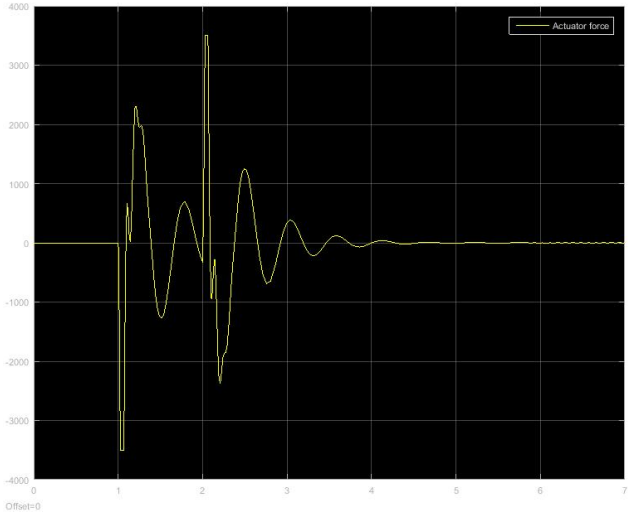

Figure 20: Actuator force for 10cm deep pothole

However considering the sprung mass displacement response, it is in fact greater than in the open-loop case. This is unexpected and suggests the although the controller did indeed minimize the suspension travel it had unintended effects of doing this by compromising the sprung mass displacement, velocity

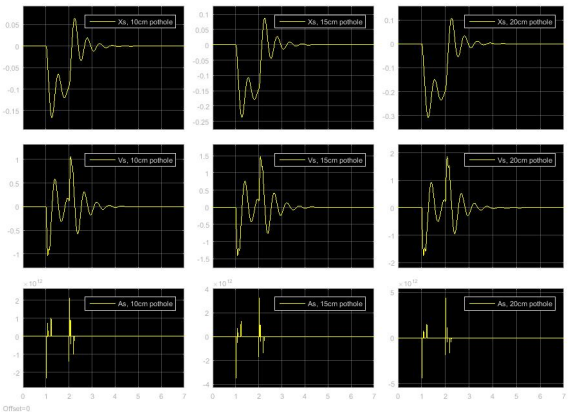

Figure 22: Closed loop sprung mass dynamics, 10, 15, 20cm deep pothole

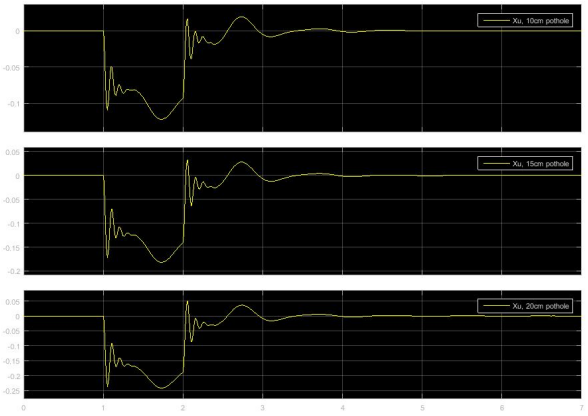

Figure 21: Closed loop tire deflection, 10, 15, 20cm deep pothole

and acceleration. Looking at Figure 21 it is clear that it is the tire displacement that received the benefit, noted by reduced peak amplitudes and decreased settling time.

3.3 Sinusoidal Bumpy

3.2.1 Varying Amplitude

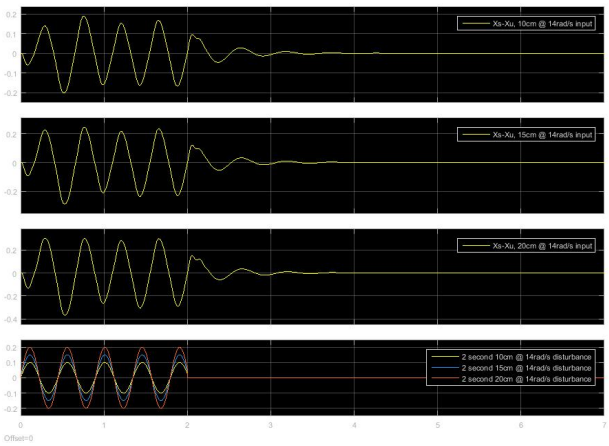

Figure 23: Closed loop sinusoidal bumpy suspension travel for 10, 15, 20cm @ 14 rad/s

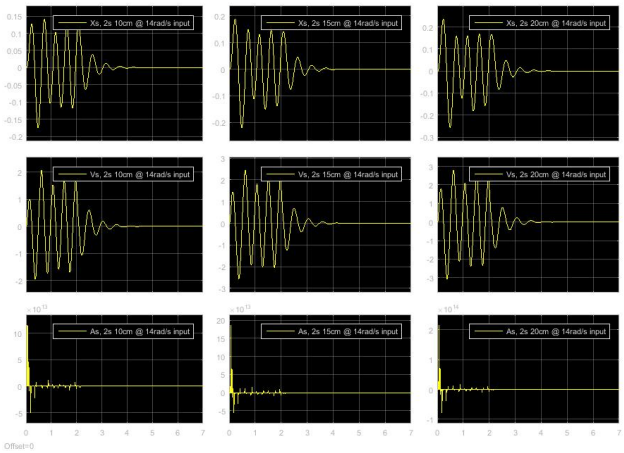

Figure 24 Closed loop sinusoidal bumpy sprung mass dynamics for 10, 15, 20cm @ 14 rad/s

Unfortunately the same thing is observed in the sinusoidal bumpy case: there is a noticeable improvement in suspension travel response yet the sprung mass dynamics are considerably worse than in the open loop case for all amplitude disturbances.

3.2.2 Varying Frequency

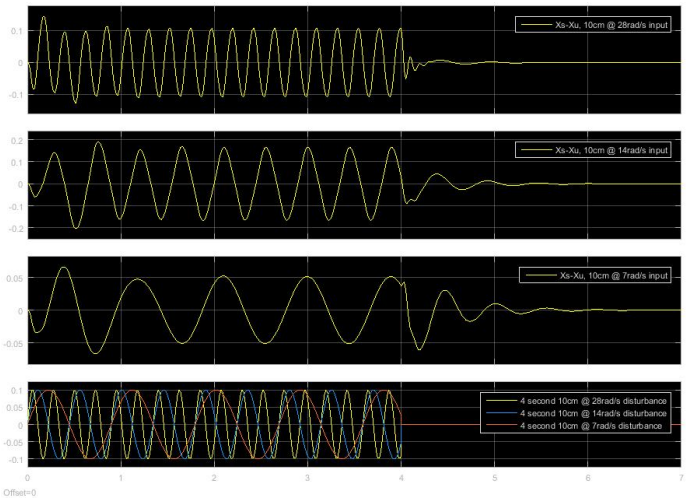

Figure 26: Closed loop sinusoidal bumpy suspension travel for 7, 14, 28 rad/s @ 10cm

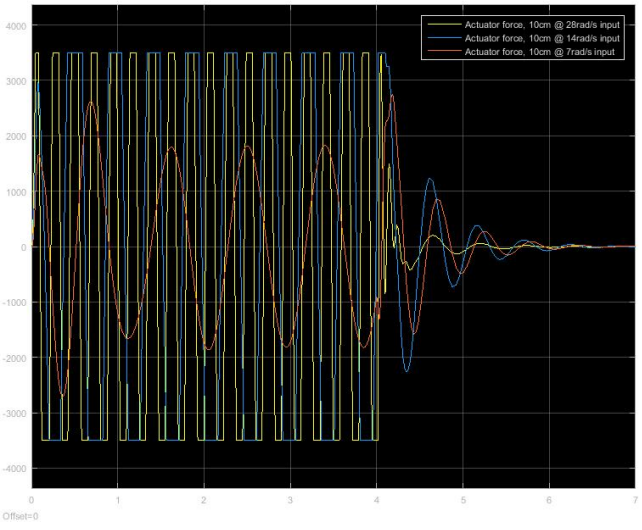

Figure 25: Closed loop sinusoidal bumpy sprung mass dynamics for 7, 14, 28 rad/s @ 10cm

Once again, it is observed that the suspension travel has an improvement over the open loop case in terms of overshoot and settling time however the trade off is increased amplitude oscillations for the sprung mass whereas the unsprung mass is visibly damped when compared to the open loop case.

Observing actuator output, the actuator reaches saturation consistently for the duration of the input disturbance for the 28 rad/s and 14 rad/s frequency input disturbances. Observing the suspension travel more closely it is possible to see that the 7 rad/s input disturbance response on suspension travel has a greater degree of improvement than the other two frequency disturbances. In either case only the settling time desired performance specification is met as the overshoot exceeds 20% in some places.

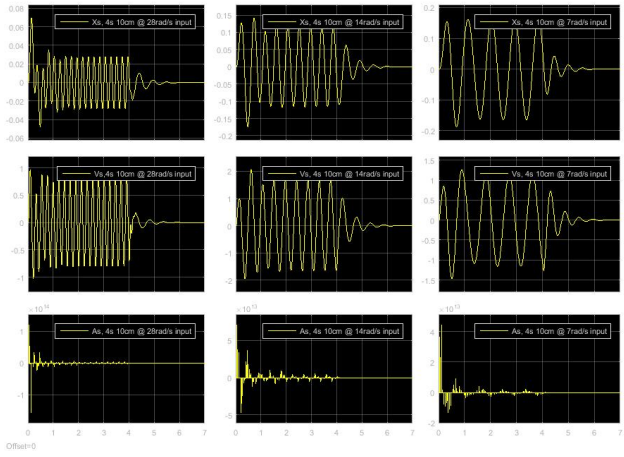

Figure 28: Closed loop sinusoidal bumpy sprung mass dynamics, 7, 14, 28 rad/s @ 10cm

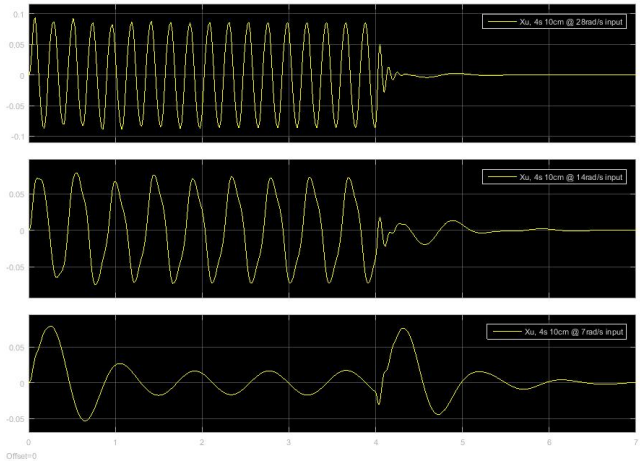

Figure 27: Closed loop sinusoidal bumpy tire deflections, 7, 14, 28 rad/s @ 10cm

3.4 Random Disturbance

For brevity random disturbance response plots are not shown but similar patterns are observed as in the other responses: reduced overshoots, increased damping, decreased settling time yet a high sprung mass displacement, velocity and acceleration. Tire deflection is

6 Conclusions and Recommendations

Simulating the obtained active control system in Simulink, the active suspension system has a clear improvement over the passive only suspension system for suspension travel. Both maximum overshoot and settling time of the suspension travel are successfully reduced to within desired performance specifications. The improved results of the suspension travel against all disturbance types strongly suggests increased rider comfort, vehicle maneuverability and safety of the active suspension system over the passive suspension system alone.

However taking a detailed look at sprung mass dynamics it becomes evident that in general the use of the actuator in fact increased sprung mass displacement, velocity and peak acceleration for all disturbance types. This suggests that the use of the PID controlled force actuator in the quarter car suspension model had unintended effects of increasing vibration of the cabin of the vehicle. It seems that the active suspension system as tuned in this report produced a vehicular response with greater control and stability in suspension travel but also one that potentially results in some rider discomfort. In some cases, sprung mass acceleration is noted to be one or two orders of magnitudes greater in the active case.

Therefore it is recommended that this effect is more closely studied such that appropriate changes can be made in either the physical parameters of the system or the controller model such that suspension travel is maintained but a reduction in unintended sprung mass dynamics is mitigated. For example

increasing the spring stiffness of the suspension system, or increasing the sprung mass over unsprung mass ratio are two ways that the force created by the actuator can have a greater effect on the tire instead of the passengers.

It is also recommended that the actuator be improved such that a force greater than 3500 N may be achieved, as this is one of the largest limiting parameters for improvement of the active suspension system. In nearly all cases was saturation met at some point during the response, for all disturbance types. Increasing the limit would result in a suspension system more capable to handle larger disturbances

Finally it is recommended that other controller types such as Linear Quadratic Regulator – an optimal controller – are considered, as is currently used in much of the state-of-the-art-research for active suspension systems [6, 7]. This mathematical formulation would allow for specific characteristics to be defined, for example minimizing sprung mass dynamics, while still achieving the objective of regulating the suspension travel at zero. In this way, a more suitable optimal controller can be quickly found without resorting to exhaustive root locus iterations, and would potentially lead to an active suspension system that offers the same increase in vehicular control but with a more comfortable and steady driving experience.

References

[1] S. M. Fayyed. (2012, Jan). *Constructing Control System for Active Suspension System* [Online]. Available: http://www.m-hikari.com/ces/ces2012/ces1-4-2012/fayyadCES1-4-2012-1.pdf

[2] A. S. Ahmed, *et al*., (2015, Dec). *PID Controller of Active Suspension System for a Quarter Car Model* [Online]. Available: http://www.ijaet.org/media/3I30-IJAET0830236-v8-iss6-pp899-909.pdf

[3] M. S. Kumar, S. Vijayarangan. (2007, Mar). *Analytical and experimental studies on active suspension system of light passenger vehicle to improve ride comfort* [Online]. Available: http://internet.ktu.lt/lt/mokslas/zurnalai/mechanika/mech_65/Senthil365.pdf

[4] K.S. Patil, *et* al., (2013, April). *Performance Evaluation of Active Suspension for Passenger Cars Using MATLAB* [Online]. Available: *http*://iosrjournals.org/iosr-jmce/papers/RDME-Volume2/RDME-12.pdf

[5] G. F. Franklin, *et al*., *Feedback Control of Dynamic Systems*, Upper Saddle River, NJ, Pearson Higher Education Inc., 2014

[6] M. M. Atef, *et al.*, (2015, Dec). *Vehicle Active Suspension System Performance using Different Control Strategies* [Online]. Available: http://www.ijettjournal.org/2015/volume-30/number-2/IJETT-V30P220.pdf

[7] K. D. Rao, S. Kumar. "Modeling and Simulation of Quarter Car Semi Active Suspension System Using LQR Controller" in P*roceedings of the 3rd International Conference on Frontiers of Intelligent Computing: Theory and Applications*, Odisha, 2014, pp. 441-448. Available: https://link.springer.com/chapter/10.1007/978-3-319-11933-5_48

Appendix A.

Eq. 8 and 11-16 with substituted values from Table 1:

$$det(A) = 21000\left(s^4 + 25.3810\,s^3 + 3258.6\,s^2 + 10833\,s + 145860\right) \quad \text{(A1)}$$

$$P(s) = \frac{410\,s^2 + 175000}{det(A)} = \frac{0.0195\,s^3 + 8.333}{\left(s^4 + 25.3810\,s^3 + 3258.6\,s^2 + 10833\,s + 145860\right)} \quad \text{(A2)}$$

$$Q(s) = \frac{-61250000\,s^2}{det(A)} = \frac{-2916.7\,s^2}{\left(s^4 + 25.3810\,s^3 + 3258.6\,s^2 + 10833\,s + 145860\right)} \quad \text{(A3)}$$

$$G_s(s) = \frac{227500\,s + 3063000000}{det(A)} = \frac{10833\,s + 145860}{\left(s^4 + 25.3810\,s^3 + 3258.6\,s^2 + 10833\,s + 145860\right)} \quad \text{(A4)}$$

$$G_t(s) = \frac{10^5\left(612.5\,s^2 + 1.763\,s + 30630\right)}{det(A)} = \frac{2916.7\,s^2 + 8.3952\,s + 145860}{\left(s^4 + 25.3810\,s^3 + 3258.6\,s^2 + 10833\,s + 145860\right)} \quad \text{(A5)}$$

$$G_s'(s) = \frac{60\,s^2 + 175000}{det(A)} = \frac{0.0029\,s^2 + 2916.7}{\left(s^4 + 25.3810\,s^3 + 3258.6\,s^2 + 10833\,s + 145860\right)} \quad \text{(A6)}$$

$$G_t'(s) = \frac{-350\,s^2}{det(A)} = \frac{-0.0167\,s^2}{\left(s^4 + 25.3810\,s^3 + 3258.6\,s^2 + 10833\,s + 145860\right)} \quad \text{(A7)}$$

Note that all characteristic equations for the above transfer functions are the same.

Appendix B

Root Contour Iteration 1

The characteristic equation can be rearranged in the following form:

$$1+k_p\frac{(m_s+m_u)s^3+b_t s^2+k_t s}{m_u m_s s^5+(k_d(m_s+m_u)+m_u b_s+b_s+b_t)s^4+(m_u k_s+b_s b_t+(k_s+k_t)m_s+k_d b_t)s^3+(2k_s b_t+k_d k_t+k_i(m_s+m_u))s^2+(b_t k_i+k_t k_s)s+k_t k_i}=0$$

Start by setting $k_i=100, k_d=100$ and varying k_p. These starting values are chosen as the controller typically will deal with distances on the order of 10^{-2} yet deal with forces on the order of 10^4; the maximum force the actuator can provide is 3500 N. In either case with sufficient root contour iterations, the initial seed values of the controller terms are arbitrary.

Using MATLAB's *rlocus()* function the following root locus plot is obtained:

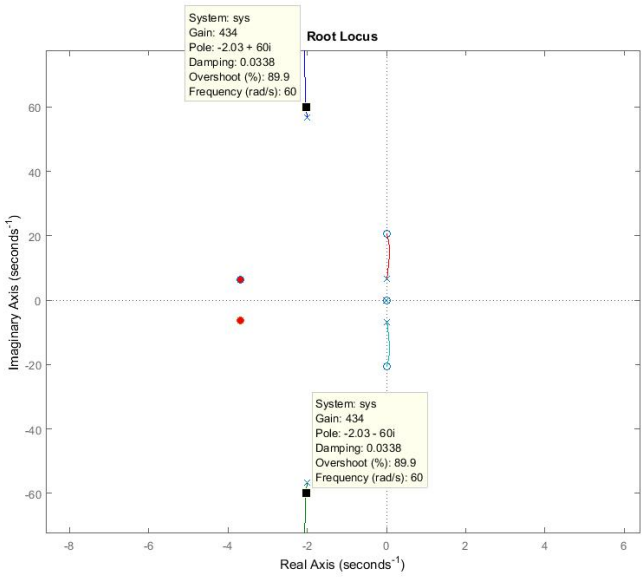

Figure 29: Root contour iteration 1 with desired closed loop poles in red

Note the RHP root locus portions indicating that any choice of k_p with the other two PID terms where they are currently will result in an unstable system. Nonetheless, proceed and take poles closest to the desired closed loop poles resulting in $k_p=22229$.

Root Contour Iteration 2

Next, keep $k_p=22229, k_i=10$ but change k_d. The characteristic equation can be rearranged in the following form:

$$1+k_d\frac{(m_s+m_u)s^4+b_t s^3+k_t s^2}{m_u m_s s^5+(m_u b_s+b_s+b_t)s^4+(m_u k_s+b_s b_t+(k_s+k_t)m_s+k_p(m_s+m_u))s^3+(2k_s b_t+b_t k_p+k_i(m_s+m_u))s^2+(k_t k_p+b_t k_i+k_t k_s)s+k_t k_i}$$

Substituting values, the resulting root locus is as follows:

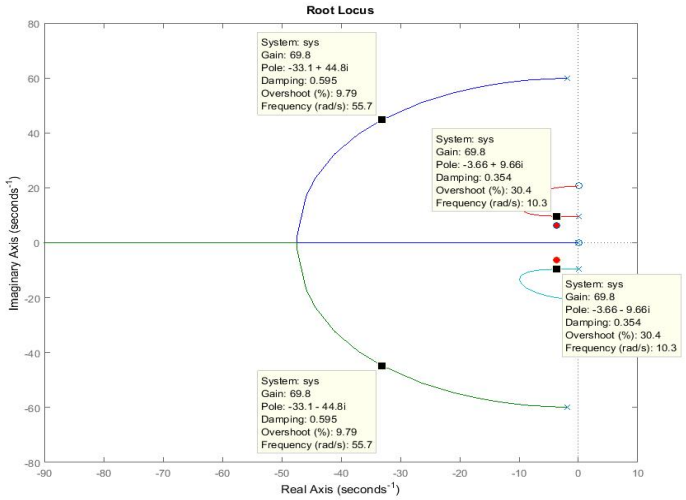

Figure 30: Root contour iteration 2 with desired closed loop poles in red

The obtained system is stable, evident as the root locus is completely in the LHP. Choose pole locations closest to the desired closed loop poles which incidentally occur nearly along the real portion of the desired closed loop poles, as in further iterations modifying the P term could lower the root locus closer to intersection with the desired closed loop poles. This results in $k_d = 3575.1$.

For brevity the rest of the root contour iterations are not shown but they follow the same procedure as above. At this time the controller response is as follows for suspension travel:

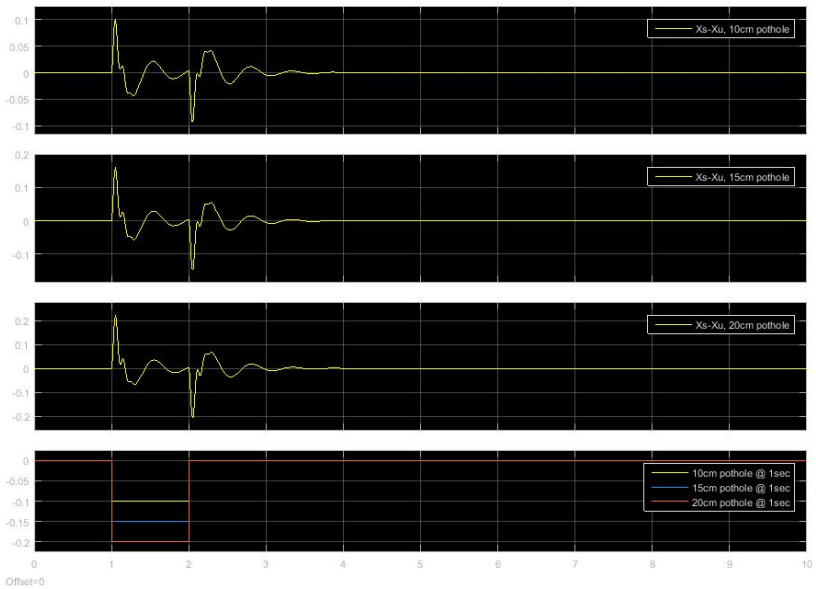

Figure 31: Active suspension travel subjected to 10, 15 and 20cm pothole @ 1 second after 2 iterations

Note an improved maximum overshoot and settling time, as well as general increased dampening observed in all signals. Results are discussed in greater detail for several disturbance types in Section 5.